

# Integration of the polyphenol and Maillard reactions into a unified abiotic pathway for humification in nature: the role of $\delta$ -MnO<sub>2</sub>

A. Jokic<sup>a</sup>, M.C. Wang<sup>b</sup>, C. Liu<sup>a</sup>, A.I. Frenkel<sup>c</sup>, P.M. Huang<sup>a,\*</sup>

<sup>a</sup>*Department of Soil Science, University of Saskatchewan, Saskatoon, Saskatchewan, Canada S7N 5A8*

<sup>b</sup>*Department and Graduate Institute of Environmental Engineering and Management, Chaoyang University of Technology, Taichung County, Taiwan*

<sup>c</sup>*Physics Department, Yeshiva University, New York, NY 10016, USA*

Received 31 August 2003; accepted 25 January 2004

(returned to author for revision 31 August 2003)

## Abstract

The Maillard reaction involving condensation reactions between sugars and amino acids is considered to be an important pathway in natural humification processes. Polyphenols in terrestrial and aquatic environments are regarded as important precursors in the formation of humic substances. In nature it is most likely that these two processes do not occur separately but rather interact with each other. We report that the ubiquitous soil mineral  $\delta$ -MnO<sub>2</sub> significantly accelerated humification processes in a system containing glucose, glycine, and catechol, at temperatures and a pH typical of natural environments. The data obtained indicate the significance of linking the polyphenol and Maillard reactions as promoted by  $\delta$ -MnO<sub>2</sub> into an integrated humification pathway.

© 2004 Elsevier Ltd. All rights reserved.

## 1. Introduction

In soils and sediments, humification processes are of principal importance in the transformation of organic molecules originating from organized structures typical of organisms (e.g., carbohydrates and proteins) to randomly polymerized, heterogeneous humic substances. Soil mineral colloids are significant in turnover of organic matter (Huang, 1995; Torn et al., 1997) and manganese (Mn) oxides are ubiquitous and widely occurring in nature (McKenzie, 1989). They frequently occur in conjunction with Fe oxides (Childs, 1975; Sidhu et al., 1977; McKeague et al., 1986), as discrete particles or partial coatings or films on soil and sediment particles (Burns and Burns, 1977; Giovanoli and Balmer, 1981; Post et al., 1982; Manceau and Combes, 1988), or as suspended particulates in water columns (Larson and Hufnal, 1980; McKenzie, 1989). Mangan-

nese oxides are powerful oxidizing agents (Shindo and Huang, 1982, 1984) and are considered the most important abiotic redox-active minerals found in many soils and sediments (Risser and Bailey, 1992). Their effectiveness as electron acceptors in a very wide range of redox reactions is unique among common soil minerals (McBride, 1989).

The Maillard reaction involving condensation reactions between sugars and amino acids (Maillard, 1913) leading to the formation of melanoidins is perceived to be an important pathway in natural humification processes (Ikan et al., 1996). The great appeal of the Maillard reaction in humification processes lies in the two proposed precursors (sugars and amino acids) being among the most abundant constituents of terrestrial and aquatic environments (Anderson et al., 1989). Further support is lent by the presence of humic substances in marine environments where carbohydrates and proteins, because of their abundance, are more probable precursors of humic substances than are lignin or phenolic polymers (Nissenbaum and Kaplan, 1972; Hedges and

\* Corresponding author. Fax: +1-306-966-6881.

E-mail address: [huangp@sask.usask.ca](mailto:huangp@sask.usask.ca) (P.M. Huang).

Parker, 1976; Ikan et al., 1996), although autooxidative crosslinking reactions between adjacent polyunsaturated fatty acids in fat molecules exposed to sunlight at the ocean surface may also contribute to the formation of humic substances in seawater (Harvey et al., 1983; Harvey and Boran, 1985). Humic substances isolated from natural environments, e.g., Lake Hula (Israel) and Lake Haruna (Japan) humic acids, have extremely similar  $^{13}\text{C}$  NMR spectra to synthetic melanoidins (Ikan et al., 1986, 1996). A major criticism of the Maillard reaction has been that it is very slow under ambient conditions (Hedges, 1988). However, it has recently been demonstrated that the action of birnessite ( $\delta\text{-MnO}_2$ ), under ambient environmental conditions, significantly accelerates the Maillard reaction and merits attention as an important abiotic pathway for the formation of humic substances (Jokic et al., 2001).

Polyphenols present in terrestrial and aquatic environments are regarded as important precursors in the formation of humic substances via processes of oxidative polymerization which take place in soils and sediments (Pal et al., 1994; Stevenson, 1994; Sparks, 1995; Huang, 2000). The polyphenol model of abiotic (mineral catalyzed) formation of humic substances has been well documented (Huang, 1995, 2000) and the catalytic action of  $\delta\text{-MnO}_2$  on mixtures of polyphenols and amino acids leading to the formation of nitrogen containing polycondensates has been demonstrated (Shindo and Huang, 1984; Wang and Huang, 1987).

Hence, both the Maillard reaction and the polyphenol model are separate, significant abiotic pathways for the formation of humic polycondensates. In nature however, it is most likely that these two pathways do not occur separately, but rather interact closely with each other, since sugars, amino acids, and polyphenols coexist in soil solutions and natural waters. It is therefore, a logical step to attempt to unify the two separate pathways, i.e., the Maillard reaction and polyphenol model, into one combined humification pathway incorporating carbohydrate, amino acid and polyphenol moieties into the humic structure as would likely occur in nature.

The objective of the present research was to examine the catalytic effect of  $\delta\text{-MnO}_2$  on the process of humification in the catechol–glucose–glycine system and to analyze humic acids (HAs) isolated from the glucose–glycine– $\delta\text{-MnO}_2$  (representative of the mineral colloid–Maillard reaction pathway), glycine–catechol– $\delta\text{-MnO}_2$  (representative of the mineral colloid–polyphenol pathway), and glucose–glycine–catechol– $\delta\text{-MnO}_2$  systems (representative of the mineral colloid–unified pathway).

## 2. Experimental methods

Mn oxides are considered the most important abiotic redox-active minerals found in many soils and sediments

(Risser and Bailey, 1992). However, naturally occurring  $\delta\text{-MnO}_2$  probably contains significant amounts of adsorbed metal ions and/or organic compounds which could interfere in studies on the abiotic transformations of organic structures. Therefore, a synthetic  $\delta\text{-MnO}_2$ , prepared according to McKenzie (1971) and known to be free of contaminants and chemicals other than those used in its preparation, was utilized in the experiments. X-ray absorption near-edge structure (XANES) spectroscopic analysis of the  $\delta\text{-MnO}_2$  showed that it contained predominantly Mn(IV) but with a significant content of Mn(III) (Jokic et al., 2001). Catechol (minimum 99%), glucose (ACS reagent grade),  $^{14}\text{C}$  uniformly labelled glucose [UL- $^{14}\text{C}$  D-glucose ( $\text{HO}^{14}\text{CH}_2[^{14}\text{CHOH}]_4^{14}\text{CHO}$ )] and glycine (Sigma Ultra grade purity) were obtained from Sigma Chemical Co. (St. Louis, MO). Distilled, deionized water (henceforth referred to as water) was used in all experiments.

The effect of  $\delta\text{-MnO}_2$  was investigated by incubating sealed 250 mL flasks, each containing 2.50 g  $\delta\text{-MnO}_2$  suspended in a solution containing an equi-molar mixture of catechol, glucose and glycine (0.05 M each) or catechol and glycine (0.05 M each) or glucose and glycine (0.05 M each) in an oscillating water bath. The concentrations of glucose and glycine used were as recommended by Hedges (1978), Benzing-Purdie et al. (1985), and Taguchi and Sampei (1986), in investigations of the Maillard reaction. The concentration of catechol used was therefore set to equal that of the glucose and glycine. The pH of the system was adjusted to an environmentally relevant initial pH of 7.00, and the final volume of the solution was set to 100 ml. The reaction mixture was incubated for 15 d at 45 °C. 45 °C is the approximate temperature of the soil surface on a day when the ambient air temperature is 25 °C (Baver, 1956; Jury et al., 1991), and is frequently encountered in tropical and subtropical regions, and even in temperate regions during the summer. Some experiments were also conducted at 25 °C with the incubation time extended to 60 d. Experiments using UL- $^{14}\text{C}$  glucose were performed only at 45 °C (15 d). Control systems containing no  $\delta\text{-MnO}_2$  only had a liquid phase since the reaction products remained in solution. Systems containing manganese had a solid phase, initially consisting only of  $\delta\text{-MnO}_2$ , but at the end of the reaction period, the solid phase consisted of unreacted  $\delta\text{-MnO}_2$  and adsorbed reaction products.

Sterile conditions were maintained by autoclaving all apparatus, water and  $\delta\text{-MnO}_2$  used, and by adding thimerosal (0.02% w/v, final volume). The absence of aerobic microbial growth was verified by culturing aliquots from reaction mixtures on Trypticase Soy Agar (TSA) plates (Dandurand and Knudsen, 1997). In addition the absence of anaerobic microorganisms was tested by culturing aliquots from selected reaction mixtures on TSA plates in a BBL (Cockeysville,

Maryland) GasPak 150™ Large Anaerobic System, i.e., in a sealed container from which all the oxygen was removed.

The procedure for experiments incorporating UL-<sup>14</sup>C glucose was as follows. The volume of the aqueous solution of UL-<sup>14</sup>C glucose was 333 μl with radioactivity of 0.15 mCi/ml. The specific activity of this solution was 7.1 mCi/mmol. The original solution was diluted to 50 ml with water. The radioactivity of the diluted solution was 50 μCi. In the experiment there were four different reaction systems (i.e., glucose–glycine–catechol–δ-MnO<sub>2</sub>, glucose–glycine–δ-MnO<sub>2</sub>, glucose–glycine–catechol, and glucose–glycine) with three replicates each. To each of the three replicates was added 2 ml of the diluted solution with radioactivity of 2 μCi (0.2817 μmol). The experimental procedure then followed that given above for the experiments using no radioactive chemicals with one difference. An autoclaved polyethylene tube (of sufficient dimensions that it leaned against the wall of the reaction vessel without danger of its contents mixing with those of the vessel) containing 10 ml of 1/3M KOH was placed in each reaction flask, prior to closing, in order to absorb any <sup>14</sup>CO<sub>2</sub> released.

### 2.1. Characterization of reaction products and isolation and analysis of humic acids

At the end of the reaction period, the solid residue from systems which contained δ-MnO<sub>2</sub> was separated from the supernatant by centrifugation at 25,000g for 40 min. The residue was repeatedly washed, dialysed against distilled, deionized water [dialysis tubing with molecular weight cut-off (MWCO) 1000] and then lyophilized. Humic acids (HAs) were isolated after 60 d reaction at 25 °C from the (1) the glucose–glycine–catechol–δ-MnO<sub>2</sub> system (representing the mineral colloid-unified pathway) and also after 15 d reaction at 45 °C from (2) the glucose–glycine–δ-MnO<sub>2</sub> (representing the mineral colloid-Maillard reaction pathway), (3) the glycine–catechol–δ-MnO<sub>2</sub> (representing the mineral colloid-polyphenol pathway), and (4) the glucose–glycine–catechol–δ-MnO<sub>2</sub> (representing the mineral colloid-unified pathway) systems. The supernatant combined with water extracts of the sediment, after centrifugation at 25000g for 40 min, was acidified to pH 1.0 by the addition of 6 M HCl to precipitate the HA. After standing for 24 h, any precipitate was separated from the supernatant by centrifugation at 2000g for 20 min. The HA polycondensates were transferred to dialysis tubing (MWCO 1000) using water and were dialysed against water until a negative chloride test (10% w/v aqueous silver nitrate) was obtained. After dialysis was completed, the precipitates were lyophilized. The quantity of HA isolated from system (1) the glucose–glycine–catechol–δ-MnO<sub>2</sub> system at 25 °C, 60 d was 7 mg; from system (2) the glucose–glycine–δ-MnO<sub>2</sub> system at 45 °C,

15 d, 15 mg; from system (3) the glycine–catechol–δ-MnO<sub>2</sub> system at 45 °C, 15 d, 325 mg; and from system (4) the glucose–glycine–catechol–δ-MnO<sub>2</sub> system at 45 °C, 15 d, 35 mg. The greatest yield of HA was obtained from the glycine–catechol–δ-MnO<sub>2</sub> system at 45 °C, 15 d. However, the glucose–glycine–catechol–δ-MnO<sub>2</sub> system provides for the incorporation of carbohydrate, amino acid and polyphenol moieties into the humic structure as would likely occur in nature. Control systems containing no δ-MnO<sub>2</sub> yielded much less HA. For example, at 45 °C, the glucose–glycine system yielded less than 1 mg HA, and the glucose–glycine–catechol control produced less than 5 mg HA. The glycine–catechol system was not run as a control.

#### 2.1.1. Visible absorbance spectroscopy

The formation of humification products was monitored by measuring changes in absorbance of the supernatants of the glucose–glycine, glucose–glycine–δ-MnO<sub>2</sub>, glucose–glycine–catechol and the glucose–glycine–catechol–δ-MnO<sub>2</sub> systems (25 °C, 60 d), and the glucose–glycine, glucose–glycine–δ-MnO<sub>2</sub>, glucose–glycine–catechol, glucose–glycine–catechol–δ-MnO<sub>2</sub> and the glycine–catechol–δ-MnO<sub>2</sub> systems (45 °C, 15 d). After centrifugation at 25000g for 40 min, spectra were recorded in the visible range from 400 to 600 nm using a Beckman DU 650 microprocessor-controlled spectrophotometer (Fullerton, CA). The pH and Eh of suspensions of the systems were measured and the Mn content of the supernatants was determined at 279.5 nm by atomic absorption (AA) spectroscopy.

The HAs obtained from the glucose–glycine–catechol–δ-MnO<sub>2</sub> system (25 °C, 60 d) and the glucose–glycine–catechol–δ-MnO<sub>2</sub> and the glycine–catechol–δ-MnO<sub>2</sub> systems (45 °C, 15 d) were also analyzed by visible absorption spectrophotometry. The ratio of the absorbance at 465 nm to that at 665 nm ( $E_4/E_6$  ratio) was calculated because it is commonly used to characterise humic substances (Stevenson, 1994). Salt concentrations can affect absorbance and  $E_4/E_6$  ratios (Ghosh and Schnitzer, 1979) as can the solvent used (Baes and Bloom, 1990) and the  $E_4/E_6$  ratio is also pH dependent (Chen et al., 1977). Therefore, 2 mg of each HA were dissolved in 10 ml of 0.05 M NaHCO<sub>3</sub>. This results in a pH of approximately 8.0 and a fixed salt concentration as recommended by Chen et al. (1977).

#### 2.1.2. Fourier Transform Infrared (FTIR) spectroscopy

The FTIR spectra of the lyophilised solid residues of the glucose–glycine–catechol–δ-MnO<sub>2</sub> system (25 °C, 60 d), and the glycine–catechol–δ-MnO<sub>2</sub>, the glucose–glycine–catechol–δ-MnO<sub>2</sub>, and the glucose–glycine–δ-MnO<sub>2</sub> systems (all at 45 °C, 15 d) were obtained using KBr disks containing 0.5% w/w sample on a Biorad 3240 SPS microprocessor-controlled spectrometer (Cambridge, MA). Samples were flushed with dry N<sub>2</sub> gas for 10–15

min prior to analysis in order to remove atmospheric CO<sub>2</sub> and moisture.

The FTIR spectra of HA samples from the glycine–catechol– $\delta$ -MnO<sub>2</sub>, the glucose–glycine–catechol– $\delta$ -MnO<sub>2</sub>, and the glucose–glycine– $\delta$ -MnO<sub>2</sub> systems (all at 45 °C, 15 d) were obtained using KBr disks containing 0.5% w/w sample as above.

#### 2.1.3. X-ray absorption near-edge structure (XANES) spectroscopy

XANES spectroscopy was employed to follow the changes in the speciation of Mn in  $\delta$ -MnO<sub>2</sub> containing systems. A sample of untreated, pure  $\delta$ -MnO<sub>2</sub> was used as control and the solid phases of the glucose–glycine–catechol– $\delta$ -MnO<sub>2</sub> systems (treated at 25 °C, 60 d and 45 °C, 15 d) were examined. XANES experiments were conducted in transmission mode at the Materials Research Laboratory (MRL) University of Illinois—Agere beam line X16-C at the National Synchrotron Light Source, Brookhaven National Laboratory, Upton, New York. The X-ray energy varied from 200 eV below to 1000 eV above the absorption K-edge of Mn ( $E_k = 6540$  eV) using a Si 111 double-crystal monochromator.

#### 2.1.4. <sup>1</sup>H solution Nuclear Magnetic Resonance (NMR) spectroscopy

<sup>1</sup>H solution NMR spectra were obtained for HAs isolated from the glycine–catechol– $\delta$ -MnO<sub>2</sub>, the glucose–glycine– $\delta$ -MnO<sub>2</sub>, and the glucose–glycine–catechol– $\delta$ -MnO<sub>2</sub> systems (all at 45 °C, 15 d) on a Bruker Avance 500 spectrometer (Bruker Analytik, Rheinstetten/Karlsruhe Germany) operating at 500.13 MHz for <sup>1</sup>H. The samples were dissolved in 2.0 ml 0.1 M NaOD/D<sub>2</sub>O under nitrogen. 256 or 2400 scans were used in obtaining the spectra, with a delay time of 1 s, and line broadening of 0.30 Hz. The water peak was used as internal standard with deuterated chloroform as external standard.

#### 2.1.5. <sup>13</sup>C Cross Polarization Magic Angle Spinning (CPMAS) Nuclear Magnetic Resonance (NMR) Spectroscopy

A sample of HA from the glycine–catechol– $\delta$ -MnO<sub>2</sub> system (45 °C, 15 d) was analyzed by <sup>13</sup>C CPMAS NMR spectroscopy on a Bruker Avance 360 DRX spectrometer (Bruker Analytik, Rheinstetten/Karlsruhe Germany) operating at 90.57 MHz for <sup>13</sup>C. Optimum spectral conditions were obtained using a contact time of 3.0 ms and relaxation delay of 2.0 s. Spinning the sample at 12 kHz eliminated sidebands but did not significantly alter spectral characteristics compared to a dissolved sample analyzed by liquid <sup>13</sup>C NMR. A 4 mm Bruker probe and phase stabilized zirconium rotor were used. Chemical shifts are expressed relative to tetramethylsilane. No background rotor effects were observed under these experimental conditions.

#### 2.1.6. Atomic Force Microscopy (AFM)

The HAs obtained from the glucose–glycine– $\delta$ -MnO<sub>2</sub>, glucose–glycine–catechol– $\delta$ -MnO<sub>2</sub> and the glycine–catechol– $\delta$ -MnO<sub>2</sub> systems (45 °C, 15 d) were compared with the standard soil HA sample of the International Humic Substances Society (IS102H). Five milligrams of each HA was dispersed in 22 ml water using ultrasonification (Sonifier Model 350, Danbury, CT) at 40 kHz and 150 watts for 2 min in an ice bath. The suspension was adjusted to pH 5.0 with 0.01 M NaOH and HNO<sub>3</sub> and diluted to 25 ml. One drop of the suspension was deposited on a watch glass and air-dried overnight at room temperature (23.5 ± 0.5 °C). The watch glass was then mounted on a magnetized stainless steel disk (12 mm diameter) with double-sided tape. The 3-dimensional AFM images were obtained under ambient conditions using the contact mode of a NanoScope<sup>TM</sup>III atomic force microscope (Digital Instruments, Inc., Santa Barbara, CA). The imaging area measured was 5  $\mu$ m × 5  $\mu$ m. The scanner type was 1881E and scanner size was 15  $\mu$ m. A silicon nitride cantilever with a spring constant of 0.12 N/m was used in the contact mode. The scanning rate was 2.2 Hz. To protect against experimental artifacts, the AFM cantilever was changed frequently. The scanning area and angle were also changed often in order to detect artifacts caused by adhesion of particles to the AFM tip. The particle size was estimated using *Section* analysis based on 30 particles after the image was enlarged.

#### 2.2. Determination of amount of <sup>14</sup>CO<sub>2</sub> released from oxidation of UL-<sup>14</sup>C glucose

At the end of the reaction period in the experiments incorporating UL-<sup>14</sup>C glucose, the KOH solution in each reaction flask was analyzed for <sup>14</sup>CO<sub>2</sub> content using a Beckman LS3801 Liquid Scintillation Counter.

### 3. Results

#### 3.1. Solution and solid phase reaction products

##### 3.1.1. Supernatants

In all the systems studied the presence of culturable, aerobic or anaerobic micro-organisms was not detected, indicating that all reactions were abiotic in nature.

Visible absorbance spectra of diluted solutions of the supernatants of the systems were recorded and the values obtained were subsequently multiplied by the dilution factor. The units are arbitrary absorbance units. The data clearly show the significant increase in browning exhibited by systems containing  $\delta$ -MnO<sub>2</sub> (both at 25 and 45 °C) compared to non- $\delta$ -MnO<sub>2</sub> containing systems (Table 1). The browning was most pronounced in systems that also contained catechol.

The addition of  $\delta$ -MnO<sub>2</sub> caused an increase in pH in all systems studied (Table 2). In contrast, the pH value of the control glucose–glycine–catechol systems (both at 25 or 45 °C) was lower than that of glucose–glycine systems. The pE + pH value of the glucose–glycine–catechol– $\delta$ -MnO<sub>2</sub> system at 25 °C was considerably lower than that of the glucose–glycine–catechol control (Table 2).

### 3.1.2. Lyophilized residues

X-ray absorption near-edge structure (XANES) spectroscopy was employed to follow the changes in the speciation of Mn in  $\delta$ -MnO<sub>2</sub>. Fig. 1 shows the Mn K-edge XANES spectra obtained, indicating Mn speciation in the different experimental systems: (a) pure  $\delta$ -MnO<sub>2</sub>, and the glucose–glycine–catechol– $\delta$ -MnO<sub>2</sub> system (b) at 25 °C (60 d), and (c) at 45 °C (15 d) all at initial pH 7.00. Compared with the glucose–glycine–catechol– $\delta$ -

MnO<sub>2</sub> system, the spectral characteristics of the glycine–catechol– $\delta$ -MnO<sub>2</sub> system at 45 °C (not shown) were very similar.

At the qualitative level the FTIR spectra of the freeze-dried residues of the glucose–glycine–catechol– $\delta$ -MnO<sub>2</sub> system (25 °C, 60 d) (Fig. 2a), the glycine–catechol– $\delta$ -MnO<sub>2</sub> system (45 °C, 15 d) (Fig. 2b), and the glucose–glycine–catechol– $\delta$ -MnO<sub>2</sub> system (45 °C, 15 d) (Fig. 2c), are very similar and differ from the FTIR spectrum of the glucose–glycine– $\delta$ -MnO<sub>2</sub> system (45 °C, 15 d) (Fig. 2d). The absence of a band at approximately 1714 cm<sup>-1</sup> (undissociated carboxyl) in (Fig. 2a–d) is consistent with the system pH's being near or above 7 (Wang and Huang, 1992) and therefore, the carboxyl groups are present in the dissociated form as absorption bands at 1394–1410 and 1585–1593 cm<sup>-1</sup> (Fig. 2a–d and Table 3).

Table 1  
Visible absorbances of supernatants in a series of reaction systems<sup>a</sup>

Reaction system	Absorbance	
	400 nm	600 nm
<i>25 °C, 60 d</i>		
Glucose–glycine	0.077±0.004	0.021±0.001
Glucose–glycine– $\delta$ -MnO <sub>2</sub>	0.367±0.006	0.067±0.002
Glucose–glycine–catechol	10.8±0.6	3.8±0.2
Glucose–glycine–catechol– $\delta$ -MnO <sub>2</sub>	90.4±3.8	37.6±1.7
<i>45 °C, 15 d</i>		
Glucose–glycine	0.342±0.018	0.103±0.006
Glucose–glycine– $\delta$ -MnO <sub>2</sub>	14.7±0.68	1.50±0.10
Glucose–glycine–catechol	5.60±0.35	2.13±0.08
Glucose–glycine–catechol– $\delta$ -MnO <sub>2</sub>	73.7±1.3	24.7±1.5
Glycine–catechol– $\delta$ -MnO <sub>2</sub>	242.0±14.7	115.0±6.9

<sup>a</sup> The glycine–catechol– $\delta$ -MnO<sub>2</sub> system was not studied at 25 °C.

Table 2  
Final pH, redox status, and Mn content of supernatants in a series of reaction systems

Treatment <sup>a</sup>	Mn ( $\mu$ g mL <sup>-1</sup> )	pH	Eh (mV)	pE + pH
<i>25 °C, 60 d</i>				
Glucose–glycine	0	7.11±0.05	411±12	14.03±0.23
Glucose–glycine– $\delta$ -MnO <sub>2</sub>	2839±71	7.68±0.09	343±10	13.47±0.26
Glucose–glycine–catechol	0	6.42±0.08	296±10	11.42±0.25
Glucose–glycine–catechol– $\delta$ -MnO <sub>2</sub>	3010±174	7.60±0.09	87±15	9.07±0.34
<i>45 °C, 15 d</i>				
Glucose–glycine	0	7.01±0.09	ND <sup>b</sup>	ND
Glucose–glycine– $\delta$ -MnO <sub>2</sub>	7803±74	7.98±0.11	ND	ND
Glucose–glycine–catechol	0	5.92±0.09	ND	ND
Glucose–glycine–catechol– $\delta$ -MnO <sub>2</sub>	3222±120	7.21±0.13	ND	ND
Glycine–catechol– $\delta$ -MnO <sub>2</sub> <sup>c</sup>	3281±141	7.66±0.15	ND	ND

<sup>a</sup> The systems were at an initially adjusted pH of 7.00.

<sup>b</sup> ND—not determined.

<sup>c</sup> The glycine–catechol– $\delta$ -MnO<sub>2</sub> system was not studied at 25 °C.

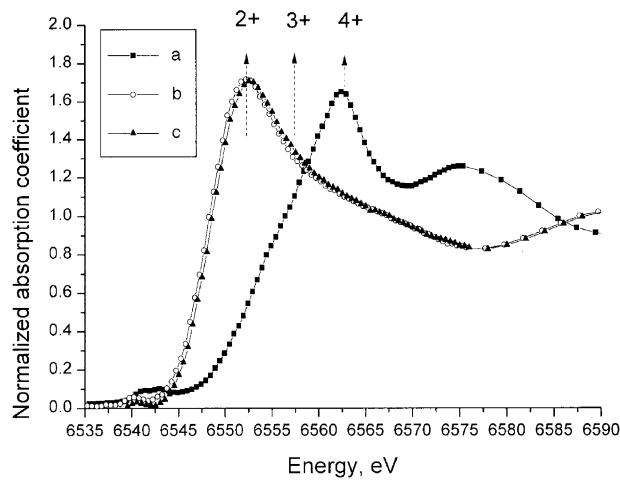


Fig. 1. XANES spectra of (a) control sample of pure  $\delta$ -MnO<sub>2</sub>, and the solid phase of the glucose–glycine–catechol– $\delta$ -MnO<sub>2</sub> system after treatment at (b) 60 d at 25 °C and (c) 15 d at 45 °C. The XANES spectrum of the glycine–catechol– $\delta$ -MnO<sub>2</sub> system (15 d at 45 °C) which is not shown is very similar to spectra (b) and (c).

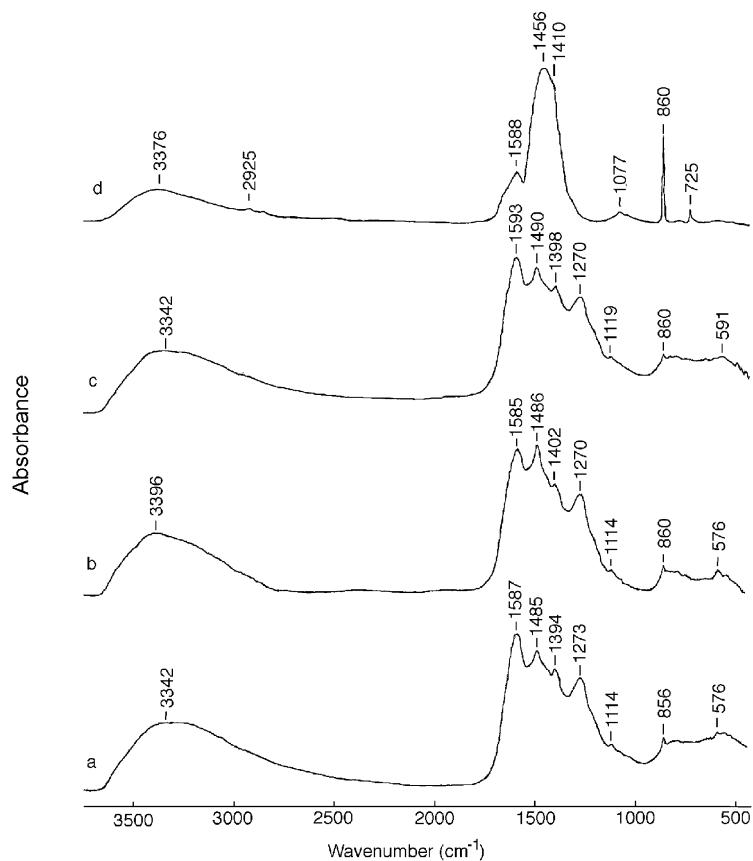


Fig. 2. FTIR spectra of the solid phase of (a) the glucose–glycine–catechol– $\delta$ -MnO<sub>2</sub> system following reaction at 25 °C for 60 d, (b) the glycine–catechol– $\delta$ -MnO<sub>2</sub>, (c) the glucose–glycine–catechol– $\delta$ -MnO<sub>2</sub> and (d) the glucose–glycine– $\delta$ -MnO<sub>2</sub> systems all following reaction at 45 °C for 15 d. Systems (a)–(d) had an initially adjusted pH of 7.00.

Table 3

Assignations of FTIR absorption bands of the solid phase of the glucose–glycine–catechol– $\delta$ -MnO<sub>2</sub>, the glycine–catechol– $\delta$ -MnO<sub>2</sub>, and the glucose–glycine– $\delta$ -MnO<sub>2</sub> systems<sup>a</sup>

(a) Glucose–glycine–catechol– $\delta$ -MnO <sub>2</sub> (25 °C) <sup>b</sup>		(b) Glycine–catechol– $\delta$ -MnO <sub>2</sub> (45 °C) <sup>c</sup>		(c) Glucose–glycine–catechol– $\delta$ -MnO <sub>2</sub> (45 °C) <sup>c</sup>		(d) Glucose–glycine– $\delta$ -MnO <sub>2</sub> (45 °C) <sup>c</sup>	
Wavenumber (cm <sup>-1</sup> )	Relative intensity	Wavenumber (cm <sup>-1</sup> )	Relative intensity	Wavenumber (cm <sup>-1</sup> )	Relative intensity	Wavenumber (cm <sup>-1</sup> )	Relative intensity
576 (vibrations of MnO <sub>6</sub> octahedra from unreacted $\delta$ -MnO <sub>2</sub> )	Weak	576 (vibrations of MnO <sub>6</sub> octahedra from unreacted $\delta$ -MnO <sub>2</sub> )	Broad	591 (vibrations of MnO <sub>6</sub> octahedra from unreacted $\delta$ -MnO <sub>2</sub> )	Weak	725 (carbohydrate interactions)	Weak
856 (carbohydrate ring semicircle stretch)	Weak	860 (carbohydrate ring semicircle stretch)	Weak	860 (carbohydrate ring semicircle stretch)	Weak	860 (carbohydrate ring semicircle stretch)	Intense, sharp
1114 (C-O stretch of carbohydrate)	Weak	1114 (C-O stretch of carbohydrate)	Weak	1119 (C-O stretch of carbohydrate)	Weak	1077 (C-O stretch of carbohydrate)	Broad, moderate
1273 (C-O stretch and in-plane C-O-H bending of COOH, C-O stretch of phenols)	Strong	1270 (C-O stretch and in-plane C-O-H bending of COOH, C-O stretch of phenols)	Strong	1270 (C-O stretch and in-plane C-O-H bending of COOH, C-O stretch of phenols)	Strong	1410 (COO <sup>-</sup> symmetric stretch)	Shoulder
1394 (OH deformation of phenols, C-H deformation of CH <sub>2</sub> and CH <sub>3</sub> , COO <sup>-</sup> antisymmetric stretching)	Strong	1402 (OH deformation of phenols, C-H deformation of CH <sub>2</sub> and CH <sub>3</sub> , COO <sup>-</sup> antisymmetric stretching)	Strong	1398 (OH deformation of phenols, C-H deformation of CH <sub>2</sub> and CH <sub>3</sub> , COO <sup>-</sup> antisymmetric stretching)	Strong	1456 (asymmetrical bending vibration of CH <sub>3</sub> and/or CH <sub>2</sub> deformation band)	Strong
1485 (symmetrical NH <sub>3</sub> <sup>+</sup> bending band)	Strong	1486 (symmetrical NH <sub>3</sub> <sup>+</sup> bending band)	Strong	1490 (symmetrical NH <sub>3</sub> <sup>+</sup> bending band)	Strong	1588 (Aromatic C=C ring stretch, asymmetric COO <sup>-</sup> stretch)	Strong
1587 (Aromatic C=C ring stretch, asymmetric COO <sup>-</sup> stretch)	Strong	1585 (Aromatic C=C, asymmetric COO <sup>-</sup> stretch)	Strong	1593 (Aromatic C=C ring stretch, asymmetric COO <sup>-</sup> stretch)	Strong	2925 (asymmetric CH <sub>2</sub> stretch)	Weak
3342 (OH stretch)	Broad, strong	3396 (OH stretch)	Broad, strong	3342 (OH stretch)	Broad, strong	3376 (OH stretch)	Broad, strong

<sup>a</sup> The assignations are based on Colthup et al. (1990), Stevenson (1994) and Silverstein and Webster (1998).<sup>b</sup> The system was treated for 60 d at 25 °C and was at an initially adjusted pH of 7.00.<sup>c</sup> The systems were treated for 15 d at 45 °C and were at an initially adjusted pH of 7.00.

### 3.2. Isolated humic acids

The highest yield of HA was obtained from the glycine–catechol– $\delta$ -MnO<sub>2</sub> system (45 °C, 15d; 325 mg). The polyphenol-amino acid system is known to yield significant amounts of humic polycondensates (Shindo and Huang, 1984). The glucose–glycine– $\delta$ -MnO<sub>2</sub> system had the lowest yield of HA (45 °C, 15 d; 15 mg), however, it is known that a substantial amount of the humified material in this system remains in the supernatant and can be isolated as fulvic acid (Jokic et al. 2001). The presence of glucose in the glucose–glycine–catechol– $\delta$ -MnO<sub>2</sub> system (45 °C, 15 d) greatly reduces the yield of HA (35 mg), although it is quite possible that substantial humified material occurs in the form of fulvic acid and remains in solution.

#### 3.2.1. Visible absorption spectroscopy

The E<sub>4</sub>/E<sub>6</sub> ratio is considered to be an indicator of the degree of humification of a system, i.e., a low ratio may indicate a higher content of aromatic structures or a higher degree of condensation, and a high ratio a greater content of aliphatic structures (Stevenson, 1994).

At 45 °C the presence of glucose markedly increases the E<sub>4</sub>/E<sub>6</sub> ratio in HA isolated from the glucose–glycine–catechol– $\delta$ -MnO<sub>2</sub> compared with the HA isolated from the glycine–catechol– $\delta$ -MnO<sub>2</sub> system (Table 4).

#### 3.2.2. FTIR analysis

FTIR analysis was performed on HAs precipitated from the supernatants of the glycine–catechol– $\delta$ -MnO<sub>2</sub> and the glucose–glycine–catechol– $\delta$ -MnO<sub>2</sub> systems. Principal bands identified include those belonging to phenols, COOH groups, and NH<sub>3</sub><sup>+</sup> from amino acids. The results are shown in Fig. 3 and Table 5.

#### 3.2.3. <sup>1</sup>H NMR analysis

<sup>1</sup>H solution NMR spectra were obtained from HAs isolated from (a) the glycine–catechol– $\delta$ -MnO<sub>2</sub> system, (b) the glucose–glycine–catechol– $\delta$ -MnO<sub>2</sub> system, and (c) the glucose–glycine– $\delta$ -MnO<sub>2</sub> system (all at 45 °C, 15 d). The aromatic region (6–8 ppm) of the glycine–catechol– $\delta$ -MnO<sub>2</sub> system is particularly pronounced relative to other signals in the spectrum. Principal components of interest in the spectra include aliphatic, carbohydrate and aromatic structures (Fig. 4 and Table 6).

Table 4

Visible absorbances and E<sub>4</sub>/E<sub>6</sub> ratios for humic acids obtained from the glucose–glycine–catechol– $\delta$ -MnO<sub>2</sub> systems, and from the glycine–catechol– $\delta$ -MnO<sub>2</sub> system

System <sup>a</sup>	A <sub>400</sub>	A <sub>465</sub>	A <sub>600</sub>	A <sub>665</sub>	E <sub>4</sub> /E <sub>6</sub>
Glucose–glycine–catechol– $\delta$ -MnO <sub>2</sub> (25 °C) <sup>b</sup>	1.62	0.98	0.35	0.22	4.46
Glucose–glycine–catechol– $\delta$ -MnO <sub>2</sub> (45 °C) <sup>c</sup>	1.91	1.04	0.28	0.14	7.43
Glycine–catechol– $\delta$ -MnO <sub>2</sub> (45 °C) <sup>c</sup>	9.00	6.70	3.20	2.30	2.91

<sup>a</sup> The systems were at an initially adjusted pH of 7.00. Two milligrams of humic acid were dissolved in 10 mL of 0.05 M NaHCO<sub>3</sub>.

<sup>b</sup> The system was treated for 60 d.

<sup>c</sup> The system was treated for 15 d.

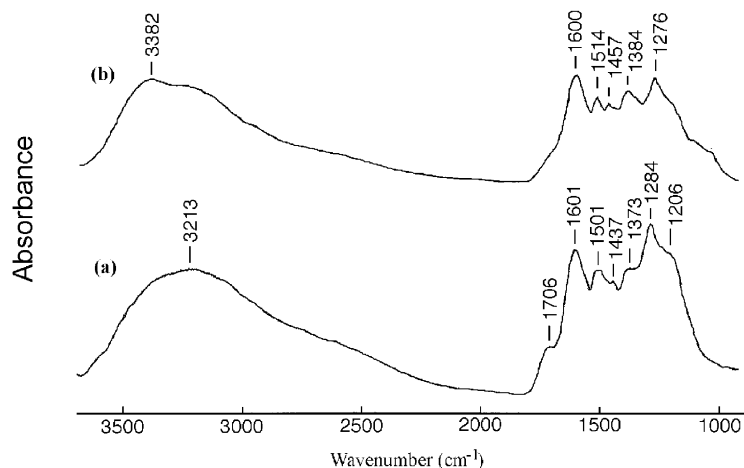


Fig. 3. FTIR spectra of isolated humic acids from: (a) the glycine–catechol– $\delta$ -MnO<sub>2</sub>, and (b) the glucose–glycine–catechol– $\delta$ -MnO<sub>2</sub> systems. The humic acids were isolated from systems with an initially adjusted pH of 7.00 and following reaction at 45 °C for 15 d.

Table 5

Assignations of FTIR absorption bands of humic acids isolated from the glycine-catechol- $\delta$ -MnO<sub>2</sub> and the glucose-glycine-catechol- $\delta$ -MnO<sub>2</sub> systems<sup>a</sup>

(a) Glycine-catechol- $\delta$ -MnO <sub>2</sub> humic acid		(b) Glucose-glycine-catechol- $\delta$ -MnO <sub>2</sub> humic acid	
Wavenumber (cm <sup>-1</sup> )	Relative intensity	Wavenumber (cm <sup>-1</sup> )	Relative intensity
1206 (C-O stretch of phenol)	Shoulder	1276 (C-O stretch and in-plane C-O-H bending of COOH, C-O stretch of phenols)	Strong
1284 (C-O stretch and in-plane C-O-H bending of COOH, C-O stretch of phenols)	Strong	1384 (OH deformation of phenols, C-H deformation of CH <sub>2</sub> and CH <sub>3</sub> , COO <sup>-</sup> antisymmetric stretching)	Moderate
1373 (OH deformation of phenols, C-H deformation of CH <sub>2</sub> and CH <sub>3</sub> , COO <sup>-</sup> antisymmetric stretching)	Shoulder	1457 (asymmetrical bending vibration of CH <sub>3</sub> and/or CH <sub>2</sub> deformation band)	Weak
1437 (OH bending of COOH)	Weak	1514 (symmetrical NH <sub>3</sub> <sup>+</sup> bending band, aromatic C=C stretch)	Weak
1501 (symmetrical NH <sub>3</sub> <sup>+</sup> bending band, aromatic C=C stretch)	Moderate	1600 (aromatic C=C ring stretch)	Strong
1601 (aromatic C=C ring stretch)	Strong		
1706 (asymmetric C=O stretch of COOH)	Shoulder	3000–2000 (NH <sub>3</sub> <sup>+</sup> stretch)	Very broad
3000–2000 (NH <sub>3</sub> <sup>+</sup> stretch)	Very broad	3382 (OH stretch)	Broad, strong
3213 (OH stretch)	Broad, strong		

<sup>a</sup> The humic acids were prepared from systems with an initially adjusted pH of 7.00 following reaction at 45 °C for 15 d. The assignations are based on Colthup et al. (1990), Stevenson (1994) and Silverstein and Webster (1998).

### 3.2.4. <sup>13</sup>C CPMAS NMR analysis

The spectrum obtained from the HA isolated from the glycine-catechol- $\delta$ -MnO<sub>2</sub> system (45 °C) is shown in Fig. 5. The spectrum broadly consists of three regions: (1) Small peaks are seen in the region <110 ppm (aliphatic including carbohydrate); (2) strong, broad peaks are found in the region of 110–160 ppm (aromatic and aromatic heterocyclic); and (3) relatively minor peaks are found at >160 ppm (carboxyl and carbonyl including amide carbon).

### 3.2.5. AFM analysis

The HAs obtained from the supernatants of the glycine-catechol- $\delta$ -MnO<sub>2</sub>, glucose-glycine- $\delta$ -MnO<sub>2</sub>, and glucose-glycine-catechol- $\delta$ -MnO<sub>2</sub> systems (45 °C, 15 d) appear as spheroidal particles in the AFM images (Fig. 6b, c and d), and are very similar to the surface features of the IHSS standard soil HA (Fig. 6a). The diameter of the IHSS standard soil HA particles ranges from ca. 50 to ca. 150 nm with an average of 85 nm (Liu and Huang, 1999). The particle size of the HAs formed in the glycine-catechol- $\delta$ -MnO<sub>2</sub> (Fig. 6b), glucose-glycine- $\delta$ -MnO<sub>2</sub> (Fig. 6c), and glucose-glycine-catechol- $\delta$ -MnO<sub>2</sub> (Fig. 6d) systems in the present study, are, respectively, in the range of ca. 60–140 nm with an average of 94 nm, in the range of ca. 50–130 nm with an average of 76 nm, and in the range of ca. 60–150 nm with an average of 98 nm. The standard errors of the measurements are  $\leq 0.27$  nm.

## 3.3. Systems containing UL-<sup>14</sup>C glucose

### 3.3.1. Evolution of <sup>14</sup>CO<sub>2</sub> released by oxidation of UL-<sup>14</sup>C glucose

The presence of  $\delta$ -MnO<sub>2</sub> or catechol in the UL <sup>14</sup>C-labelled glucose-glycine-catechol system markedly increased the evolution of <sup>14</sup>CO<sub>2</sub> (Table 7). The sequence of the amounts of <sup>14</sup>CO<sub>2</sub> released from the reaction systems was glucose-glycine-catechol- $\delta$ -MnO<sub>2</sub> > glucose-glycine- $\delta$ -MnO<sub>2</sub> > glucose-glycine-catechol > glucose-glycine and the differences were significant (Table 7).

## 4. Discussion

### 4.1. Solution and solid phase reaction products

#### 4.1.1. Supernatants

The ability of  $\delta$ -MnO<sub>2</sub> to accelerate the polymerization of polyphenols and polycondensation of polyphenols and amino acids is well known (e.g., Shindo and Huang, 1982, 1984). Its role in accelerating the Maillard (polycondensation) reaction between sugars and amino acids has recently been noted (Jokic et al., 2001). Therefore, in the glucose-glycine-catechol- $\delta$ -MnO<sub>2</sub> system a complex process apparently occurs, i.e., a simultaneous polymerisation reaction involving catechol and polycondensation reactions of (i) glucose and glycine, (ii) catechol and glycine and (iii) glucose, glycine,

and catechol. Reduction of Mn(IV) and Mn(III) (from  $\delta$ -MnO<sub>2</sub>) to Mn(II) and release of Mn(II) into the supernatant also occurs (Table 2). The polymerization and polycondensation products (humic substances) formed in the glycine–catechol– $\delta$ -MnO<sub>2</sub> system had the highest absorbances in the visible range 400–600 nm of the systems studied (Table 1). This is attributed to the

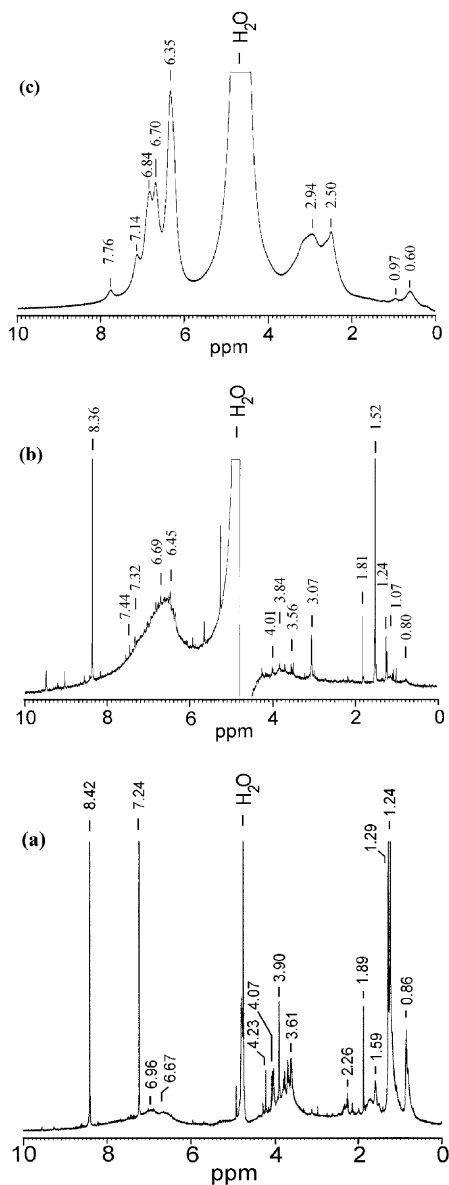


Fig. 4. <sup>1</sup>H solution NMR spectra of isolated humic acids from: (a) the glucose–glycine–catechol– $\delta$ -MnO<sub>2</sub> system (20 mg), (b) the glycine–catechol– $\delta$ -MnO<sub>2</sub> system (20 mg), and (c) the glucose–glycine– $\delta$ -MnO<sub>2</sub> system (10 mg). All samples were dissolved in 2.0 ml NaOD/D<sub>2</sub>O. All humic acids were precipitated from systems with an initially adjusted pH of 7.00 and treated at 45 °C for 15 d.

apparent inhibiting effect of glucose on polymerization/polycondensation reactions in the glucose–glycine–catechol– $\delta$ -MnO<sub>2</sub> system, and/or the increased content of aliphatic structures in the glucose–glycine–catechol– $\delta$ -MnO<sub>2</sub> system which absorb less intensely at 400 and 600 nm. The products formed in the glycine–catechol– $\delta$ -MnO<sub>2</sub> system are therefore apparently more aromatic in nature (cf. Section 3.2.1 visible absorption spectroscopy, Table 4; Section 3.2.3 <sup>1</sup>H NMR analysis, Fig. 4 and Table 6; Section 3.2.4 <sup>13</sup>C CPMAS NMR spectroscopic data, Fig. 5).

Since the pE + pH value is a function of O<sub>2</sub> concentration, it is a measure of the redox status of a system (Lindsay, 1979). Polymerization of catechol generates protons whereas the reduction of Mn(IV) and Mn(III) consumes protons. Polycondensation reactions produce water. In the absence of  $\delta$ -MnO<sub>2</sub> the pH in the glucose–glycine–catechol systems both at 25 and at 45 °C was lower (Table 2). In the presence of  $\delta$ -MnO<sub>2</sub> the pH at the end of the reaction increases, because of the net effect of these concomitant processes, i.e., reduction of Mn and the polymerisation/polycondensation reactions. At pH 7, the amino group of glycine is still partially protonated (isoelectric point for glycine is 6.06). As the pH in the systems increases during the course of reaction there is increasing deprotonation of the glycine molecules which may also provide protons for reduction of Mn(IV) and Mn(III). Reduction of Mn with subsequent consumption of protons and increase in pH was the dominant process in all systems containing  $\delta$ -MnO<sub>2</sub>. At 45 °C the amount of Mn released to the solution from the glucose–glycine– $\delta$ -MnO<sub>2</sub> system was the highest of all the systems containing  $\delta$ -MnO<sub>2</sub> (Table 2). This may be due to partial adsorption of Mn(II) on the surface of the solid phase of the glycine–catechol– $\delta$ -MnO<sub>2</sub> and glucose–glycine–catechol– $\delta$ -MnO<sub>2</sub> systems. Adsorption of reaction products on the surface of the glycine–catechol– $\delta$ -MnO<sub>2</sub> and glucose–glycine–catechol– $\delta$ -MnO<sub>2</sub> systems could also prevent further polymerisation/polycondensation reactions from occurring.

#### 4.1.2. Lyophilized residue

Several features in the XANES spectra in the energy region between 6545 and 6565 eV (Fig. 1) indicate distinct changes in the oxidation state of Mn in samples (b) and (c) compared to sample (a). The energies corresponding to the positions of Mn(II), Mn(III), and Mn(IV), indicated by the assignments (2+), (3+) and (4+), are in good agreement with those obtained from several reference Mn-containing compounds (Manceau et al., 1992). The XANES data indicate that there was substantial reduction of Mn(IV) to lower Mn oxidation states, Mn(II) and Mn(III), (Fig. 1b and c). This supports the atomic absorption (AA) spectroscopic data (Table 2) which indicates dissolution of a substantial amount of Mn in the liquid phase of the glucose–gly-

Table 6

Interpretation of the  $^1\text{H}$  solution NMR spectra of the humic acid isolated from (a) glucose–glycine–catechol– $\delta\text{-MnO}_2$ , (b) glycine–catechol– $\delta\text{-MnO}_2$ , and (c) glucose–glycine– $\delta\text{-MnO}_2$  systems<sup>a</sup>

(a) Glucose–glycine–catechol– $\delta\text{-MnO}_2$ humic acid		(b) Glycine–catechol– $\delta\text{-MnO}_2$ humic acid		(c) Glucose–glycine– $\delta\text{-MnO}_2$ humic acid	
Chemical shift (ppm)	Assignment	Chemical shift (ppm)	Assignment	Chemical shift (ppm)	Assignment
0.86	terminal methyl groups of methylene chains	0.80	terminal methyl groups of methylene chains	0.60	terminal methyl groups
				0.97	terminal methyl groups of methylene chains
1.24, 1.29	protons on methyl groups of highly branched aliphatic structures and/or methyl in lactate	1.07	protons on methyl groups of highly branched aliphatic structures		
1.59	methylene of alicyclic compounds	1.24	methyl in lactate		
1.89	acetate	1.52	methylene of alicyclic compounds		
2.26	Protons attached to aliphatic carbons which are alpha or attached to, e.g., a carboxyl group	1.81	acetate	2.50, 2.94	Protons attached to aliphatic carbons which are alpha or attached to electronegative structures (e.g. a carboxyl group or an aromatic ring)
		3.07	aromatic amines		
3.61	methylaryl ether	3.56	methylaryl ether		
3.90	methylaryl ether or carbohydrate HCO	3.84	methylaryl ether or carbohydrate HCO		
4.07	methine in lactate	4.01	methine in lactate		
4.23	methylene attached to ester	6.45, 6.69, 7.32, 7.44	amide, sterically unhindered aromatic protons, pyrrole, and indole NH groups	6.35, 6.70, 6.84, 7.14, 7.76	amide, sterically unhindered aromatic protons, pyrrole, and indole NH groups
6.67, 6.96	amide, sterically unhindered aromatic protons, pyrrole, and indole NH groups				
7.24	probable artifact				
8.42	formate	8.36	formate		

<sup>a</sup> All humic substances were prepared from systems with an initially adjusted pH of 7.00 following reaction at 45 °C for 15 d. The assignments are based on Wilson et al. (1988), Malcolm (1990), and Silverstein and Webster (1998).

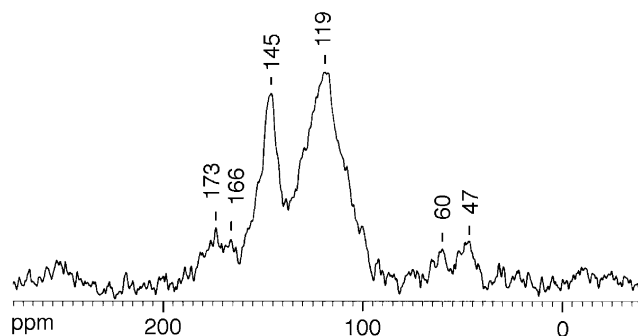


Fig. 5.  $^{13}\text{C}$  CPMAS NMR spectrum of humic acid isolated from the supernatant of the glycine–catechol– $\delta\text{-MnO}_2$  system with an initially adjusted pH of 7.00 and treated at 45 °C for 15 d.

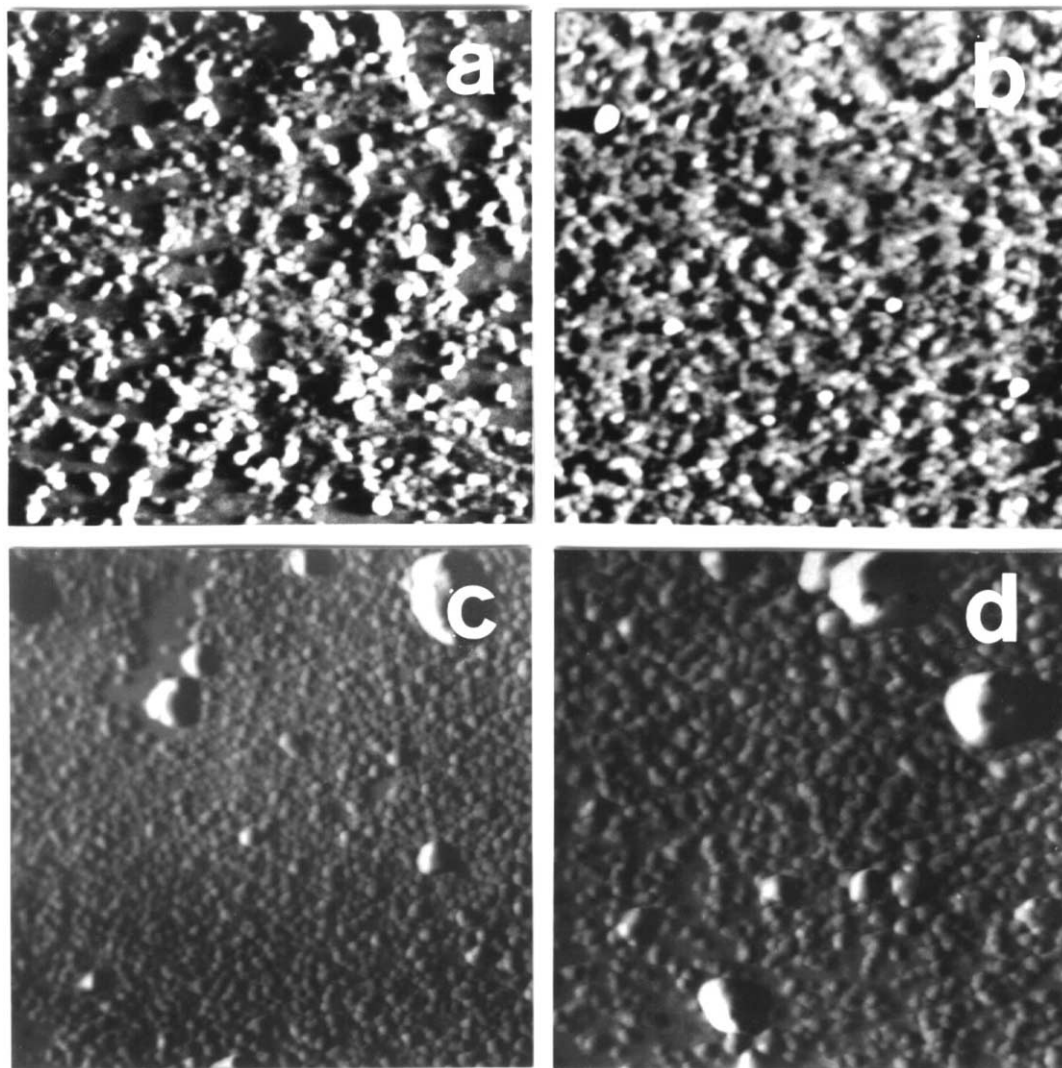


Fig. 6. AFM images of (a) International Humic Substances Society standard soil humic acid and the polycondensates formed by (b) the glycine-catechol- $\delta$ -MnO<sub>2</sub> (c) glucose-glycine- $\delta$ -MnO<sub>2</sub>, and (d) glucose-glycine-catechol- $\delta$ -MnO<sub>2</sub> systems at an initially adjusted pH of 7.00, and temperature of 45 °C for 15 d. Each image has dimensions of 5×5  $\mu$ m.

cine-catechol- $\delta$ -MnO<sub>2</sub> systems, both at 25 and 45 °C, and the glycine-catechol- $\delta$ -MnO<sub>2</sub> system at 45 °C. Therefore, the glucose-glycine-catechol- $\delta$ -MnO<sub>2</sub> system undergoes a complex redox reaction, with reduction of Mn(IV) to Mn(III) and Mn(II) (Fig. 1) and the partial entry of Mn(II) into the supernatant (Table 2). There is a concomitant polycondensation reaction between the polyphenol and glycine (cf. Section 3.2.4 <sup>13</sup>C CPMAS NMR analysis, Fig. 5) as postulated by Wang and Huang (1987). Further, particularly at 45 °C, there is oxidation of glucose catalyzed by  $\delta$ -MnO<sub>2</sub> (it is known that active Mn oxide can oxidize glucose forming carboxylic acid derivatives as described by Bose et al., 1959) probably initially forming  $\alpha$ -dicarbonyl com-

pounds that can then couple with glycine, and undergo the Strecker degradation leading to the formation of heterocyclic N compounds (Ho, 1996). The rising pH during the course of the reaction causes increasing deprotonation of glycine and promotes attack on carbonyl functional groups. A further complex polycondensation reaction may occur involving glucose, glycine and catechol together as catalyzed by  $\delta$ -MnO<sub>2</sub>.

#### 4.2. Isolated humic acids

It appears that the presence of carbohydrate inhibits the formation of HA since yields of humic acids from the sugar-amino acid-polyphenol- $\delta$ -MnO<sub>2</sub> system are

Table 7  
The release of  $^{14}\text{CO}_2$  from UL- $^{14}\text{C}$  glucose in selected reaction systems<sup>a</sup>

Reaction conditions				$^{14}\text{CO}_2$ released Bq
Glucose	Glycine	Catechol	$\delta\text{-MnO}_2$	
+ <sup>b</sup>	+	+	+	38.8 a
+	+	- <sup>c</sup>	+	28.3 b
+	+	+	-	22.4 c
+	+	-	-	14.0 d
LSD				0.6

<sup>a</sup> The systems were treated for 15 d at 45 °C and were at an initially adjusted pH of 7.00. The data with different lower case letters in a column between reaction conditions are significantly different at 5% level by least significant difference (LSD) test.

<sup>b</sup> In the presence.

<sup>c</sup> In the absence.

considerably lower than in the amino acid–polyphenol– $\delta\text{-MnO}_2$  system. Although the polyphenol–amino acid– $\delta\text{-MnO}_2$  system had the highest yield of HA, it should be noted that in many natural environments carbohydrates and amino acids are ubiquitous, as are mineral colloids, and therefore the polyphenol–amino acid–sugar– $\delta\text{-MnO}_2$  system is the closest approximation to actual environmental conditions. Other factors affecting HA yield may include the age, surface area and reactivity of the synthetic  $\delta\text{-MnO}_2$  used.

#### 4.2.1. Visible absorption spectroscopy

The  $E_4/E_6$  ratio for the HA isolated from the glucose–glycine–catechol– $\delta\text{-MnO}_2$  system (Table 4) at 25 °C (4.46) is quite close to the value of 4.3 quoted by Schnitzer (1972) for several natural HAs. At 45 °C the presence of glucose increases the  $E_4/E_6$  ratio and hence the aliphatic nature of the HA (Table 4). The HA from the glycine–catechol– $\delta\text{-MnO}_2$  system appears to be quite aromatic in nature and this observation is confirmed by  $^1\text{H}$  and  $^{13}\text{C}$  CPMAS NMR spectroscopy (cf Sections 3.2.3 and 3.2.4, Figs. 4 and 5 and Table 6).

#### 4.2.2. FTIR analysis

The HA isolated from the glycine–catechol– $\delta\text{-MnO}_2$  system (Fig. 3a and Table 5) has a pronounced shoulder at around  $1706\text{ cm}^{-1}$  (C=O of COOH) compared to the HA from the glucose–glycine–catechol– $\delta\text{-MnO}_2$  system (Fig. 3b and Table 5). This is attributed to the presence of undissociated carboxylic acid groups.

#### 4.2.3. $^1\text{H}$ NMR analysis

Peaks in the aliphatic and carbohydrate region (from ~0.8 to 4.2 ppm) of the HA isolated from the glucose–glycine–catechol– $\delta\text{-MnO}_2$  system (Fig. 4a) are more pronounced than those in the aromatic region (from ~6

to 8 ppm) whereas in the glycine–catechol– $\delta\text{-MnO}_2$  system HA (Fig. 4b) the most prominent resonances occur in the aromatic region. The spectrum of the glucose–glycine–catechol– $\delta\text{-MnO}_2$  system (Fig. 4a) resembles published spectra of naturally occurring HAs (Wilson, 1981; Wilson et al., 1983, 1988). Individual sharp peaks that are observed in both spectra (Fig. 4a and b) are distinct from other broad  $^1\text{H}$  resonances and their existence is ascribed to the presence of low molecular weight species originally covalently bonded to the humic polycondensate macromolecule, which have become separated by base hydrolysis and/or oxidation (Wilson et al., 1988). For example, sharp peaks that are observed at 1.24, or 1.29 and 1.81 or 1.89 ppm, are assigned (Wilson et al., 1988) to lactate and acetate, respectively, while those at 8.36 or 8.42 ppm are assigned to formate. The HA from the glycine–catechol– $\delta\text{-MnO}_2$  system (Fig. 4b) exhibits strong signals in the region 6–8 ppm. Amide, pyrrole and indole groups are known to absorb in this region (Silverstein and Webster, 1998). The possible presence of amide carbon is also indicated by the presence of a peak at 173 ppm in the  $^{13}\text{C}$  CPMAS spectrum (Fig. 5). The  $^1\text{H}$  NMR spectrum (Fig. 4b) is in agreement with the  $^{13}\text{C}$  CPMAS NMR spectrum of the same HA (Fig. 5) since the strong signals in the region 6–8 ppm (Fig. 4b) correspond to prominent peaks at 119 and 145 ppm ascribed to aromatic and phenolic moieties (Fig. 5).

The spectrum of the HA from the glucose–glycine– $\delta\text{-MnO}_2$  system (Fig. 4c) is qualitatively different from Fig. 4a and b. There are only weak signals in the aliphatic region that are ascribed to terminal methyl groups but strong broad peaks are present in the region from ~2 to 4 (carbohydrate) and 6 to 8 (aromatic C and N structures) ppm. The broad water peak obscures any signals which may be present in the region of 4.0–5.5 ppm.

#### 4.2.4. $^{13}\text{C}$ CPMAS NMR analysis

The spectrum of HA isolated from the glycine–catechol– $\delta\text{-MnO}_2$  system (45 °C) has several interesting features (Fig. 5). The peak at 47 ppm may arise from amino acid carbon (Malcolm, 1989) or from methoxyl groups which can produce signals in the region of 46–59 ppm according to Mendham et al. (2002). The peak at 60 ppm corresponds to the carbon in  $\text{CH}_2\text{OH}$  groups (Malcolm, 1989). It is known that  $\delta\text{-MnO}_2$  promotes the ring cleavage of polyphenols (Wang and Huang, 1992; Majcher et al., 2000), which results in the formation of open-chain moieties. The strong peak in the aromatic region with a maximum at 119 ppm is attributed to protonated aromatic carbon, and/or aromatic carbon ortho to oxygen-substituted aromatic carbon (Hatcher et al., 1980; Malcolm, 1989). The strong peak with maximum at 145 ppm arises from phenolic or aromatic amine carbon (Hatcher et al., 1980). The peaks at 166

and 173 ppm are ascribed to carboxyl and possibly amide carbon groups incorporated into the polycondensate. Carboxyl groups could arise from the oxidation by  $\delta$ -MnO<sub>2</sub> of CH<sub>2</sub>OH groups formed by the ring cleavage of catechol caused by the action of  $\delta$ -MnO<sub>2</sub> (Majcher et al., 2000) and from amino acid. The HA formed in the glycine–catechol– $\delta$ -MnO<sub>2</sub> system is highly aromatic in nature, which is in agreement with the E<sub>4</sub>/E<sub>6</sub> ratio (Table 4) and <sup>1</sup>H NMR analysis (Fig. 4b). The spectrum (Fig. 5) is very similar to the <sup>13</sup>C CPMAS NMR spectrum of a diluvial HA from Japan (Kramer et al., 2001). Therefore  $\delta$ -MnO<sub>2</sub> promotes the polycondensation reaction between polyphenol and glycine leading to the formation of high molecular weight products as postulated by Wang and Huang (1987).

#### 4.2.5. AFM analysis

The average particle size of the humic macromolecules formed varied with the reaction system (Fig. 6a–d). In particular, the humic macromolecules formed in the glucose–glycine– $\delta$ -MnO<sub>2</sub> system were, on the average, smaller than those formed in the glycine–catechol– $\delta$ -MnO<sub>2</sub>, and glucose–glycine–catechol– $\delta$ -MnO<sub>2</sub> systems (Fig. 6b, c, and d). Apparently, the presence of catechol in the reaction system resulted in an increase in the size of humic macromolecules formed in the supernatant. Some massive particles evident in the AFM images of the HA samples from the glucose–glycine– $\delta$ -MnO<sub>2</sub>, and glucose–glycine–catechol– $\delta$ -MnO<sub>2</sub> systems (Fig. 6c and d) may be attributed to the metal-humic complexes in the samples due to the incomplete purification of the HA samples.

#### 4.3. Systems containing UL-<sup>14</sup>C glucose

The decarboxylation of glucose in the Maillard reaction may involve the ring cleavage of glucose and/or decarboxylation from side chain C. This needs to be clarified by using glucose with <sup>14</sup>C labelled on either side chain C or ring structure C in the reaction systems. It is known that oxidation of simple sugars such as glucose by active manganese dioxide leads to the formation of carboxylic acids (Bose et al. 1959). A comparison of Table 1 and Table 7 indicates that the humification (browning) effect upon addition of  $\delta$ -MnO<sub>2</sub> to the glucose–glycine–catechol system (45 °C, 15 d) was more striking than the decarboxylation of glucose. It is noted from Table 1 that the absorbance of the glucose–glycine–catechol system (45 °C, 15 d) both at 400 nm and 600 nm increased by an order of magnitude in the presence of  $\delta$ -MnO<sub>2</sub>. However, from Table 7, the addition of  $\delta$ -MnO<sub>2</sub> to the glucose–glycine–catechol system (45 °C, 15 d) led to a less than twofold increase in the amount of <sup>14</sup>CO<sub>2</sub> released, i.e., from 22.4 Bq to 38.8 Bq.

## 5. Conclusions

The role of polyphenols in influencing the Maillard reaction involving condensation reactions between sugars and amino acids and the catalytic effect of  $\delta$ -MnO<sub>2</sub> on these humification processes which could occur in soils and related environments was previously not known. Soil mineral colloids are significant in the turnover of organic matter (Huang, 1995; Torn, 1997) and manganese oxides are one of the most widespread mineral constituents of soils and sediments (McKenzie, 1989). Such mineral colloids could catalyze the reaction between polyphenols, sugars and amino acids, by a process of mineral surface sorption and condensation resulting in the accelerated formation of humic substances in nature. During the process the adsorbed substrates would be protected against microbial action.

The present study shows that in the presence of glucose, glycine, and catechol, the accelerating effect of  $\delta$ -MnO<sub>2</sub> on polymerization and polycondensation processes, resulting in the formation of humic substances, at environmentally relevant temperatures and pH is dramatic. Isolated humic materials had complex spectral and physical characteristics similar to naturally occurring soil humic materials. Further, the data indicate that the presence of glucose perturbed polycondensation reactions between glycine and catechol possibly leading to the formation of more aliphatic structures. The E<sub>4</sub>/E<sub>6</sub> ratio in the glucose–glycine–catechol– $\delta$ -MnO<sub>2</sub> system, a measure of the degree of humification in a system, also increased upon increasing reaction temperature. Although the glycine–catechol– $\delta$ -MnO<sub>2</sub> system produced the highest yield of humic acids of all the systems studied, the glucose–glycine–catechol– $\delta$ -MnO<sub>2</sub> system is more representative because of the ubiquity of carbohydrates in many natural environments. Therefore, the role of carbohydrates in natural abiotic humification mechanisms, in particular, merits further attention.

The promoting effect of  $\delta$ -MnO<sub>2</sub> on the system consisting of carbohydrate, amino acid and polyphenol is a complex process involving surface mineral sorption and condensation and points to a linking of the polyphenol and Maillard reactions into an integrated humification pathway—a significant advancement in the understanding of natural humification processes in soils and sediments.

*Associate Editor—George Wolff*

## Acknowledgements

We are grateful to two anonymous referees for their comments, which helped to improve this manuscript.

This study was supported by a Discovery Grant (GP 2383-Huang) from the Natural Sciences and Engineering Research Council of Canada. The beamline X16C at the NSLS is supported in part by the U.S. Department of Energy through the Seitz Materials Research Laboratory (DEFG02-91-ER45439). The NSLS is supported by the Divisions of Materials and Chemical Sciences of the U.S. Department of Energy.

## References

- Anderson, H.A., Bick, W., Hepburn, A., Stewart, M., 1989. Nitrogen in Humic Substances. In: Hayes, M.H.B., MacCarthy, P., Malcolm, R.L., Swift, R.S. (Eds.), *Humic Substances II In Search of Structure*. Wiley-Interscience, Chichester, pp. 223–253.
- Baes, A.U., Bloom, P.R., 1990. Fulvic acid ultraviolet-visible spectra: influence of solvent and pH. *Soil Science Society of America Journal* 54, 1248–1254.
- Baver, L.D., 1956. *Soil Physics*, 3rd Edn. John Wiley and Sons, New York.
- Benzing-Purdie, L.M., Ripmeester, J.A., Ratcliffe, C.I., 1985. Effects of temperature on Maillard reaction products. *Journal of Agriculture and Food Chemistry* 33, 31–33.
- Bose, J.L., Foster, A.B., Stacey, M., Webber, J.M., 1959. Action of manganese dioxide on simple carbohydrates. *Nature* 184, 1301–1302.
- Burns, R.G., Burns, V.M., 1977. Mineralogy. In: Glasby, G.P. (Ed.), *Marine Manganese Deposits*. Elsevier, Amsterdam, NL, pp. 185–248.
- Chen, Y., Senesi, N., Schnitzer, M., 1977. Information provided on humic substances by  $E_4/E_6$  ratios. *Soil Science Society of America Journal* 41, 352–358.
- Childs, C.W., 1975. Composition of iron-manganese concretions from some New Zealand soils. *Geoderma* 13, 141–152.
- Colthup, N.B., Daly, L.H., Wiberley, S.E., 1990. *Introduction to Infrared and Raman Spectroscopy*. Academic Press Inc. Harcourt Brace Jovanovich, Boston, MA.
- Dandurand, L.-M.C., Knudsen, G.R., 1997. Sampling microbes from the rhizosphere and phyllosphere. In: Hurst, C.J. (Ed.), *Manual of Environmental Microbiology*. American Society for Microbiology, Washington, D.C., pp. 391–399.
- Ghosh, K., Schnitzer, M., 1979. UV and visible absorption spectroscopic investigations in relation to macromolecular characterizations in humic substances. *Journal of Soil Science* 30, 735–745.
- Giovanoli, R., Balmer, B., 1981. A new synthesis of hollandite. A possibility for immobilization of nuclear waste. *Chimia* 35, 53–55.
- Harvey, G.R., Boran, D.A., Chesal, L.A., Tokar, J.M., 1983. The structure of marine fulvic and humic acids. *Marine Chemistry* 12, 119–132.
- Harvey, G.R., Boran, D.A., 1985. Geochemistry of humic substances in seawater. In: Aiken, G.R., McKnight, D.M., Wershaw, R.L., MacCarthy, P. (Eds.), *Humic Substances in Soil, Sediment and Water: Geochemistry, Isolation and Characteristics*. Wiley-Interscience, New York, pp. 233–247.
- Hatcher, P.G., Rowan, R., Mattingly, M.A., 1980.  $^1\text{H}$  and  $^{13}\text{C}$  NMR of marine humic acids. *Organic Geochemistry* 2, 77–85.
- Hedges, J.I., 1978. The formation and clay mineral reactions of melanoidins. *Geochimica et Cosmochimica Acta* 42, 69–76.
- Hedges, J.I., 1988. Polymerization of humic substances in natural environments. In: Frimmel, F.H., Christman, R.F. (Eds.), *Humic Substances and Their Role in the Environment*. John Wiley and Sons, Chichester, UK, pp. 45–58.
- Hedges, J.I., Parker, P.L., 1976. Land-derived organic matter in surface sediments from the Gulf of Mexico. *Geochimica et Cosmochimica Acta* 40, 1019–1029.
- Ho, C.-T., 1996. Thermal generation of Maillard aromas. In: Ikan, R. (Ed.), *The Maillard Reaction: Consequences for the Chemical and Life Sciences*. John Wiley and Sons, Chichester, UK, pp. 27–53.
- Huang, P.M., 1995. The role of short-range ordered mineral colloids in abiotic transformations of organic components in the environment. In: Huang, P.M., Berthelin, J., Bollag, J.-M., McGill, W.B., Page, A.L. (Eds.), *Environmental Impact of Soil Component Interactions: Vol. 1 Natural and Anthropogenic Organics*. CRC/Lewis Publishers, Boca Raton, FL, pp. 135–167.
- Huang, P.M., 2000. Abiotic catalysis. In: Sumner, M.E. (Ed.), *Handbook of Soil Science*. CRC Press, Boca Raton, FL, pp. B303–B332.
- Ikan, R., Rubinsztain, Y., Aizenshtat, Z., Pugmire, R., Anderson, L.L., Woolfenden, W.R., 1986. Carbon-13 cross polarized magic-angle samples spinning nuclear magnetic resonance of melanoidins. *Organic Geochemistry* 9, 199–212.
- Ikan, R., Rubinsztain, Y., Nissenbaum, A., Kaplan, I.R., 1996. Geochemical aspects of the Maillard Reaction. In: Ikan, R. (Ed.), *The Maillard Reaction: Consequences for the Chemical and Life Sciences*. John Wiley and Sons, Chichester, UK, pp. 1–25.
- Jokic, A., Frenkel, A.I., Vairavamurthy, M., Huang, P.M., 2001. Birnessite catalysis of the Maillard reaction: its significance in natural humification. *Geophysical Research Letters* 28, 3899–3902.
- Jury, W.A., Gardner, W.R., Gardner, W.H., 1991. *Soil Physics*, 5th Edn. John Wiley and Sons, Inc, New York.
- Kramer, R.W., Kujawinski, E.B., Zang, X., Green-Church, K.B., Jones, R.B., Freitas, M.A., Hatcher, P.G., 2001. Studies of the structure of humic substances by electrospray ionization coupled to a quadrupole-time of flight (QQ-TOF) mass spectrometer. In: Ghabbour, E.A., Davies, G. (Eds.), *Humic Substances: Structures, Models and Functions*. Royal Society of Chemistry, Cambridge, UK, pp. 95–107.
- Larson, R.A., Hufnagel Jr., J.M., 1980. Oxidative polymerization of dissolved phenols by soluble and insoluble inorganic species. *Limnology and Oceanography* 25, 505–512.
- Lindsay, W.L., 1979. *Chemical Equilibria in Soils*. John Wiley and Sons, New York.
- Liu, C., Huang, P.M., 1999. Atomic force microscopy of pH, ionic strength, and cadmium effects on surface features of humic acid. In: Ghabbour, E.A., Davies, G. (Eds.), *Understanding Humic Substances: Advances in Methods, Properties, and Applications*. Royal Society of Chemistry, Cambridge, England, pp. 87–99.
- Maillard, L.C., 1913. Formation de matieres humiques par action de polypeptides sur sucres. *Comptes Rendus del' Académie des Sciences* 156, 148–149.

- Majcher, E.M., Chorover, J., Bollag, J.-M., Huang, P.M., 2000. Evolution of CO<sub>2</sub> during birnessite-induced oxidation of <sup>14</sup>C-labeled catechol. *Soil Science Society of America Journal* 64, 157–163.
- Malcolm, R.L., 1989. Applications of solid-state <sup>13</sup>C NMR spectroscopy to geochemical studies of humic substances. In: Hayes, M.H.B., MacCarthy, P., Malcolm, R.L., Swift, R.S. (Eds.), *Humic Substances II. In Search of Structure*. Wiley-Interscience, John Wiley and Sons, Chichester, UK, pp. 339–372.
- Malcolm, R.L., 1990. The uniqueness of humic substances in each of soil, stream and marine environments. *Analytica Chimica Acta* 232, 19–30.
- Manceau, A., Combes, J.M., 1988. Structure of Mn and Fe oxides and oxyhydroxides. A topological approach by EXAFS. *Physics and Chemistry of Minerals* 15, 283–295.
- Manceau, A., Gorshkov, A.I., Drits, V.A., 1992. Structural chemistry of Mn, Fe, Co, and Ni in manganese hydrous oxides: Part I. Information from XANES spectroscopy. *American Mineralogist* 77, 1133–1143.
- McBride, M.B., 1989. Surface chemistry of soil minerals. In: Dixon, J.B., Weed, S.B. (Eds.), *Minerals in Soil Environments*, 2nd Edn. SSSA, Madison, WI, pp. 35–88.
- McKeague, J.A., Cheshire, M.V., Andreux, F., Berthelin, J., 1986. Organo-mineral complexes in relation to pedogenesis. In: Huang, P.M., Schnitzer, M. (Eds.), *Interactions of Soil Minerals with Natural Organics and Microbes*. SSSA Spec. Publ. 17. SSSA, Madison, WI, pp. 549–592.
- McKenzie, R.M., 1971. The synthesis of birnessite, cryptomelane, and some other oxides and hydroxides of manganese. *Mineral Magazine* 38, 493–502.
- McKenzie, R.M., 1989. Manganese oxides and hydroxides. In: Dixon, J.B., Weed, S.B. (Eds.), *Minerals in Soil Environments*, 2nd ed. SSSA, Madison, WI, pp. 439–465.
- Mendham, D.S., Mathers, N.J., O'Connell, A.M., Grove, T.S., Saffigna, P.G., 2002. Impact of land-use on soil organic matter quality in south-western Australia—characterization with <sup>13</sup>C CP/MAS NMR spectroscopy. *Soil Biology & Biochemistry* 34, 1669–1673.
- Nissenbaum, A., Kaplan, J.R., 1972. Chemical and isotopic evidence for the *in situ* origin of marine humic substances. *Limnology and Oceanography* 17, 570–582.
- Pal, S., Bollag, J.-M., Huang, P.M., 1994. Role of abiotic and biotic catalysts in the transformation of phenolic compounds through oxidative coupling reactions. *Soil Biology & Biochemistry* 26, 813–820.
- Post, J.E., Von Dreele, R.B., Buseck, P.R., 1982. Symmetry and cation displacements in hollandites. Structure refinements of hollandite, cryptomelane, and priderite. *Acta Crystallographica B* 38, 1056–1065.
- Risser, J.A., Bailey, G.W., 1992. Spectroscopic study of surface redox reactions with manganese oxides. *Soil Science Society of America Journal* 56, 82–88.
- Schnitzer, M., 1972. Chemical, spectroscopic, and thermal methods for the classification and characterization of “humic substances”. *Proc. Intern. Meeting Humic Substances, Wageningen* 193–310.
- Shindo, H., Huang, P.M., 1982. Role of Mn (IV) oxide in abiotic formation of humic substances in the environment. *Nature* 298, 363–365.
- Shindo, H., Huang, P.M., 1984. Significance of Mn(IV) oxide in abiotic formation of organic nitrogen complexes in natural environments. *Nature* 308, 57–58.
- Sidhu, P.S., Seghal, J.L., Sinha, M.K., Randhawa, N.S., 1977. Composition and mineralogy of iron-manganese concretions from some soils of the Indo-Gangetic plain in northwest India. *Geoderma* 18, 241–249.
- Silverstein, R.M., Webster, F.X., 1998. *Spectrometric Identification of Organic Compounds*. John Wiley & Sons Inc, New York, NY.
- Sparks, D.L., 1995. *Environmental Soil Chemistry*. Academic Press, San Diego, CA.
- Stevenson, F.J., 1994. *Humus Chemistry—Genesis, Composition, Reactions*, 2nd edn. John Wiley and Sons, New York, NY.
- Taguchi, K., Sampei, Y., 1986. The formation and clay mineral and CaCO<sub>3</sub> association reactions of melanoidins. *Organic Geochemistry* 10, 1081–1089.
- Torn, M.S., Trumbore, S.E., Chadwick, O.A., Vitousek, P.M., Hendicks, D.M., 1997. Mineral control of soil organic carbon storage and turnover. *Nature* 317, 613–616.
- Wang, M.C., Huang, P.M., 1987. Polycondensation of pyrogallol and glycine and the associated reactions as catalysed by birnessite. *Science of the Total Environment* 62, 435–442.
- Wang, M.C., Huang, P.M., 1992. Significance of Mn(IV) oxide in the abiotic ring cleavage of pyrogallol in natural environments. *Science of the Total Environment* 113, 147–157.
- Wilson, M.A., 1981. Applications of nuclear magnetic resonance spectroscopy to the study of the structure of soil organic matter. *Journal of Soil Science* 32, 167–186.
- Wilson, M.A., Collins, P.J., Tate, K.R., 1983. <sup>1</sup>H-nuclear magnetic resonance study of a soil humic acid. *Journal of Soil Science* 34, 297–304.
- Wilson, M.A., Collins, P.J., Malcolm, R.L., Perdue, E.M., Cresswell, P., 1988. Low molecular weight species in humic and fulvic fractions. *Organic Geochemistry* 12, 7–12.